

Supplementary Information

Resettable Skin Interfaced Microfluidic Sweat Collection Devices with Chemesthetic Hydration Feedback

Jonathan T. Reeder^{1,2}, Yeguang Xue^{3,4}, Daniel Franklin², Yujun Deng^{3,4,5}, Jungil Choi^{1,2,6}, Olivia Prado⁷, Robin Kim⁷, Claire Liu⁷, Justin Hanson⁸, John Ciraldo⁹, Amay J. Bandonkar^{1,2}, Siddharth Krishnan¹⁰, Alexandra Johnson⁶, Emily Patnaude⁶, Raudel Avila^{3,4}, Yonggang Huang^{1,3,4}, John A. Rogers^{1,2,4,5,11,12}*

¹Department of Materials Science and Engineering, McCormick School of Engineering, Northwestern University, Evanston, IL 60208, USA

²Center for Bio-Integrated Electronics, Northwestern University, Evanston, IL 60208, USA

³Department of Civil and Environmental Engineering, McCormick School of Engineering, Northwestern University, Evanston, IL 60208, USA

⁴Department of Mechanical Engineering, McCormick School of Engineering, Northwestern University, Evanston, IL 60208, USA

⁵State Key Laboratory of Mechanical System and Vibration, Shanghai Jiao Tong University, Shanghai, 200240, China

⁶School of Mechanical Engineering, Kookmin University, Seoul 02707, Republic of Korea

⁷Department of Biomedical Engineering, McCormick School of Engineering, Northwestern University, Evanston, IL 60208, USA

⁸Department of Biology, Feinberg School of Medicine, Northwestern University, Chicago IL 60611 USA

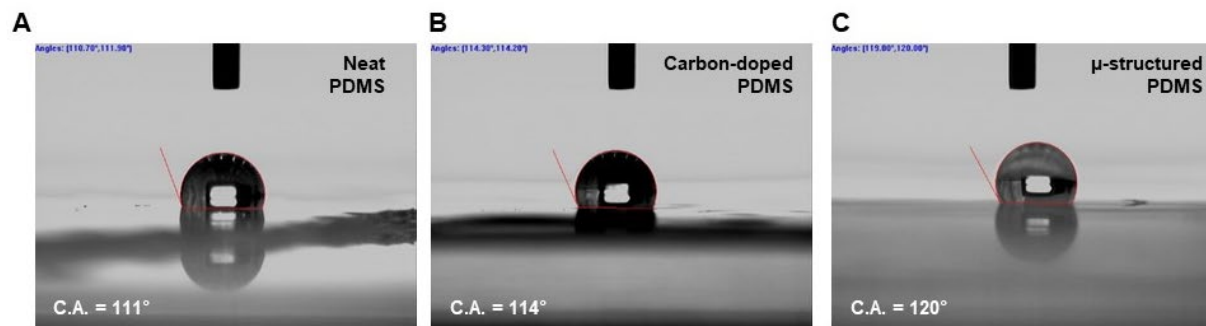
⁹Micro/Nano Fabrication Facility, Northwestern University, Evanston, IL 60208, USA

¹⁰Department of Materials Science and Engineering and Frederick Seitz Materials Research Laboratory, University of Illinois at Urbana-Champaign, Urbana, IL 61801, USA

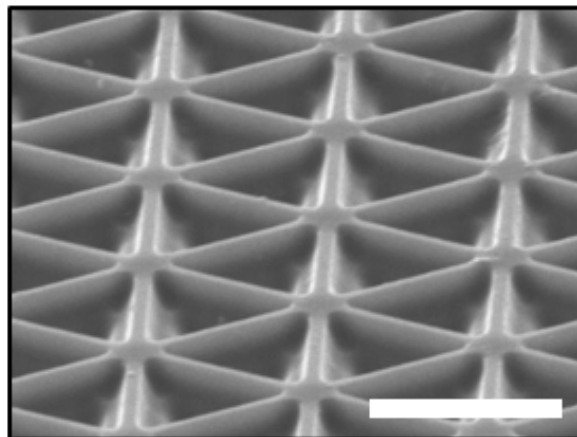
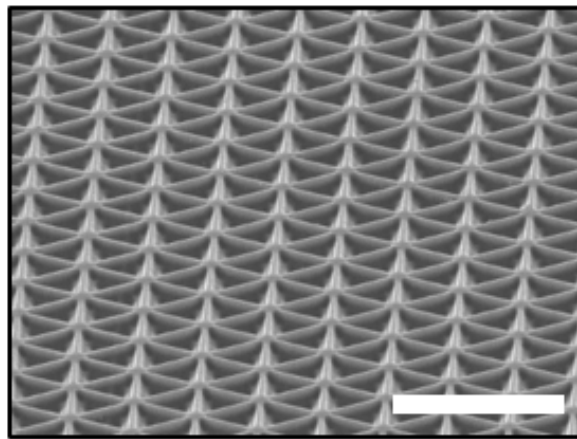
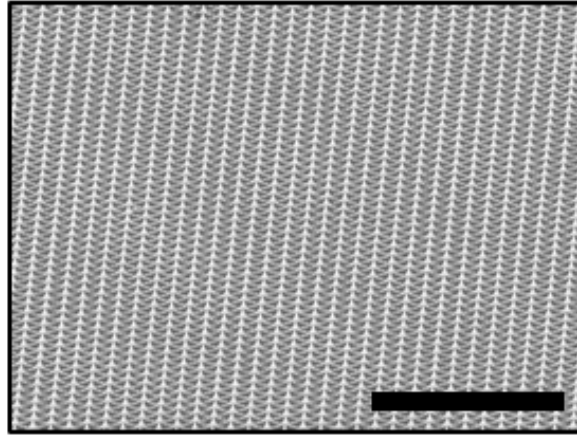
¹¹Departments of Chemistry, Electrical Engineering, Computer Science, McCormick School of Engineering, Northwestern University, Evanston, IL 60208, USA

¹²Departments of Neurological Surgery, Feinberg School of Medicine, Northwestern University, Chicago IL 60611 USA

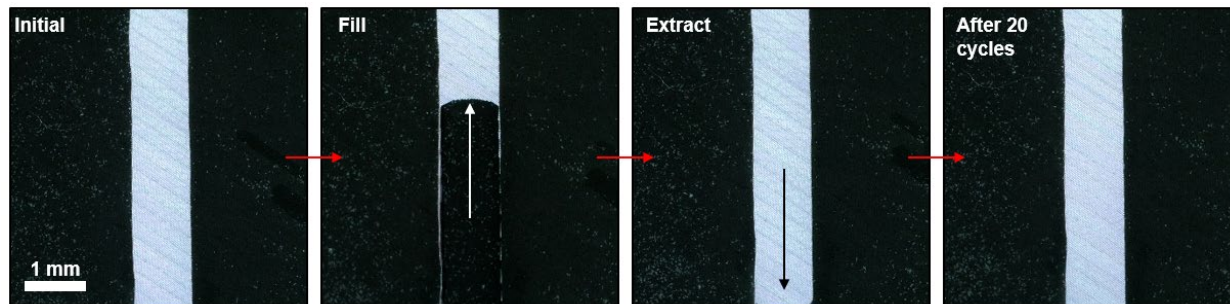
Corresponding author: jrogers@northwestern.edu



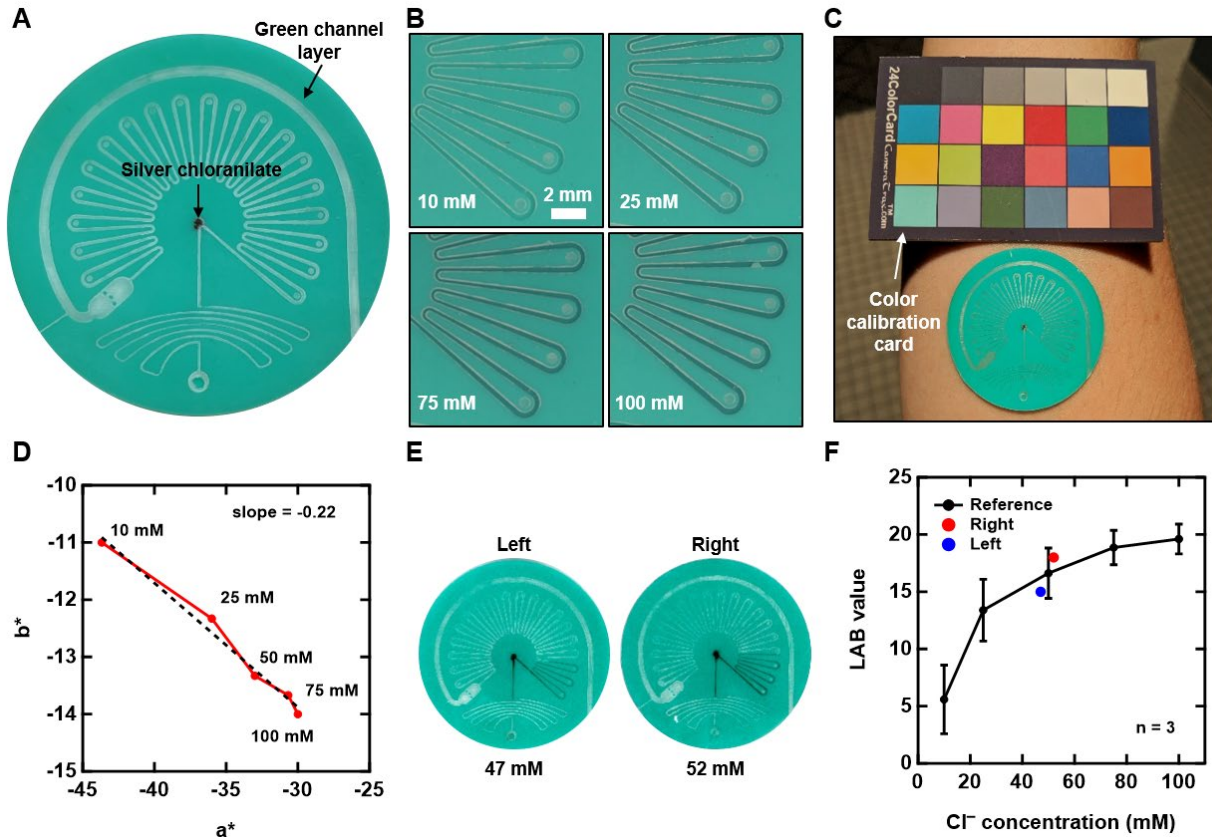
Supplementary Figure 1. Contact angle of PDMS surfaces. A) Neat PDMS. B) PDMS doped with carbon black. C) Microstructured PDMS.



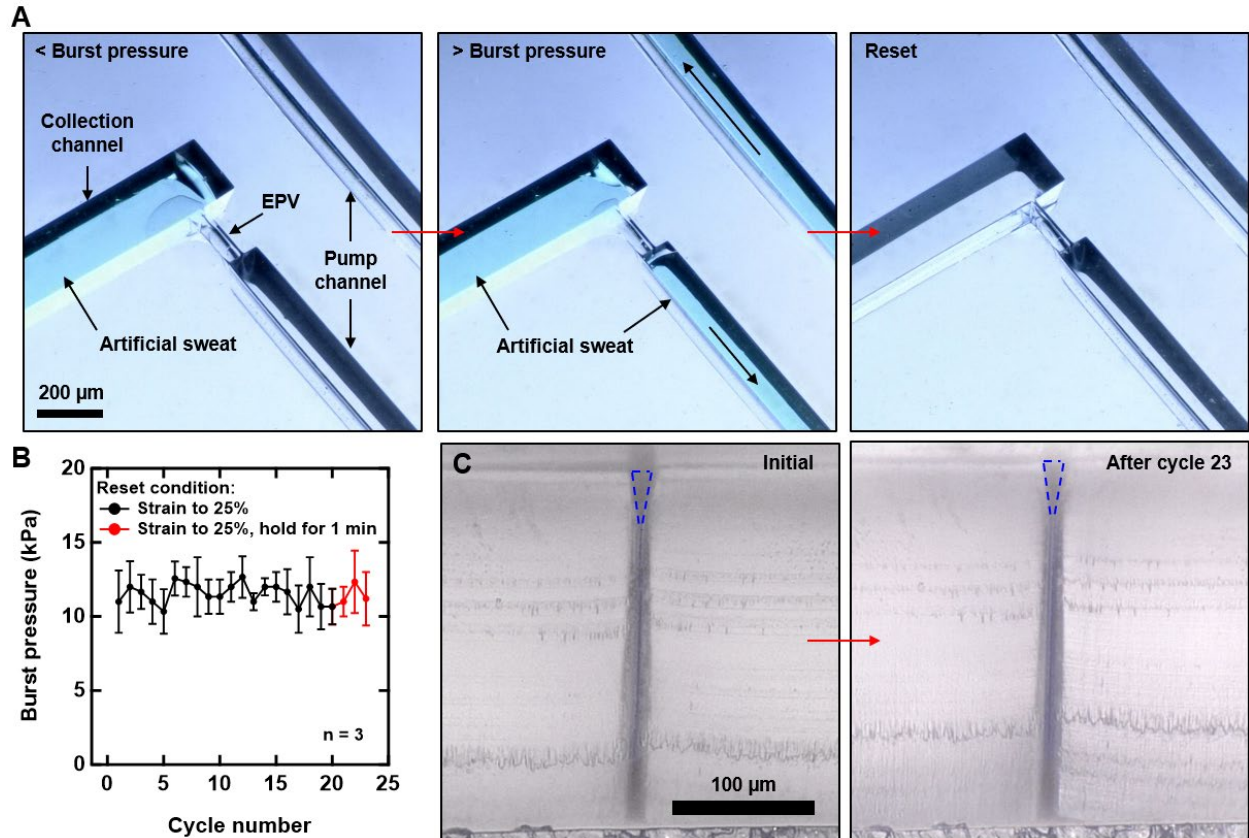
Supplementary Figure 2. Fluid indicator molds. Scanning electron microscopy of epoxy molds fabricated from a master photoresist mold formed via grayscale lithography. Scale bars: 200, 50, 20 μm (top to bottom)



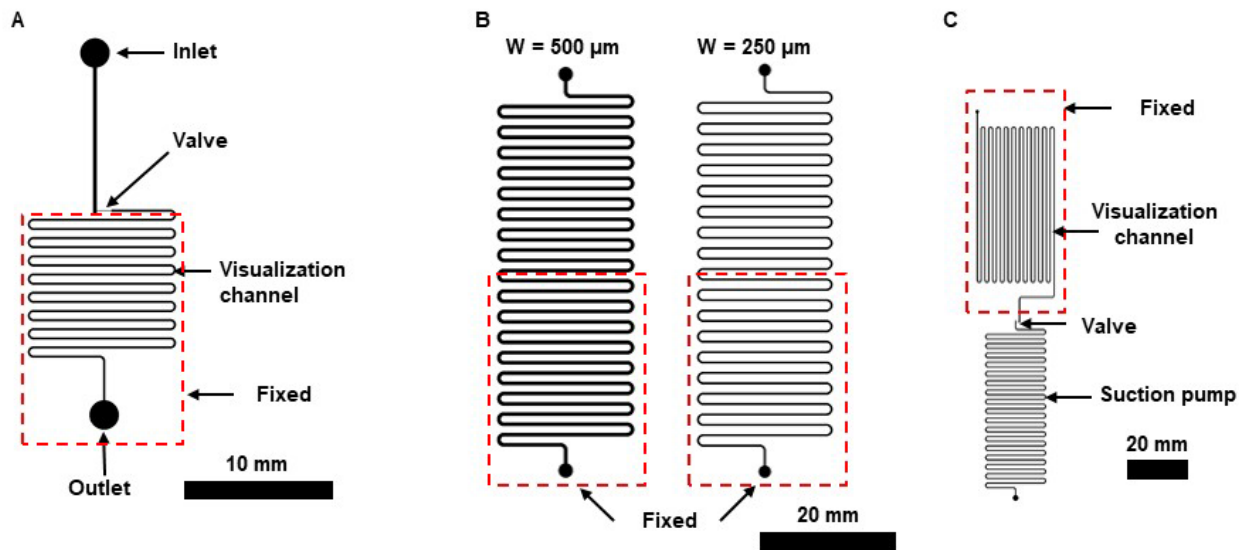
Supplementary Figure 3. Microstructural optics repeatability. Effect of cyclic filling and extraction of 50 mM NaCl. Scale bar: 1 mm.



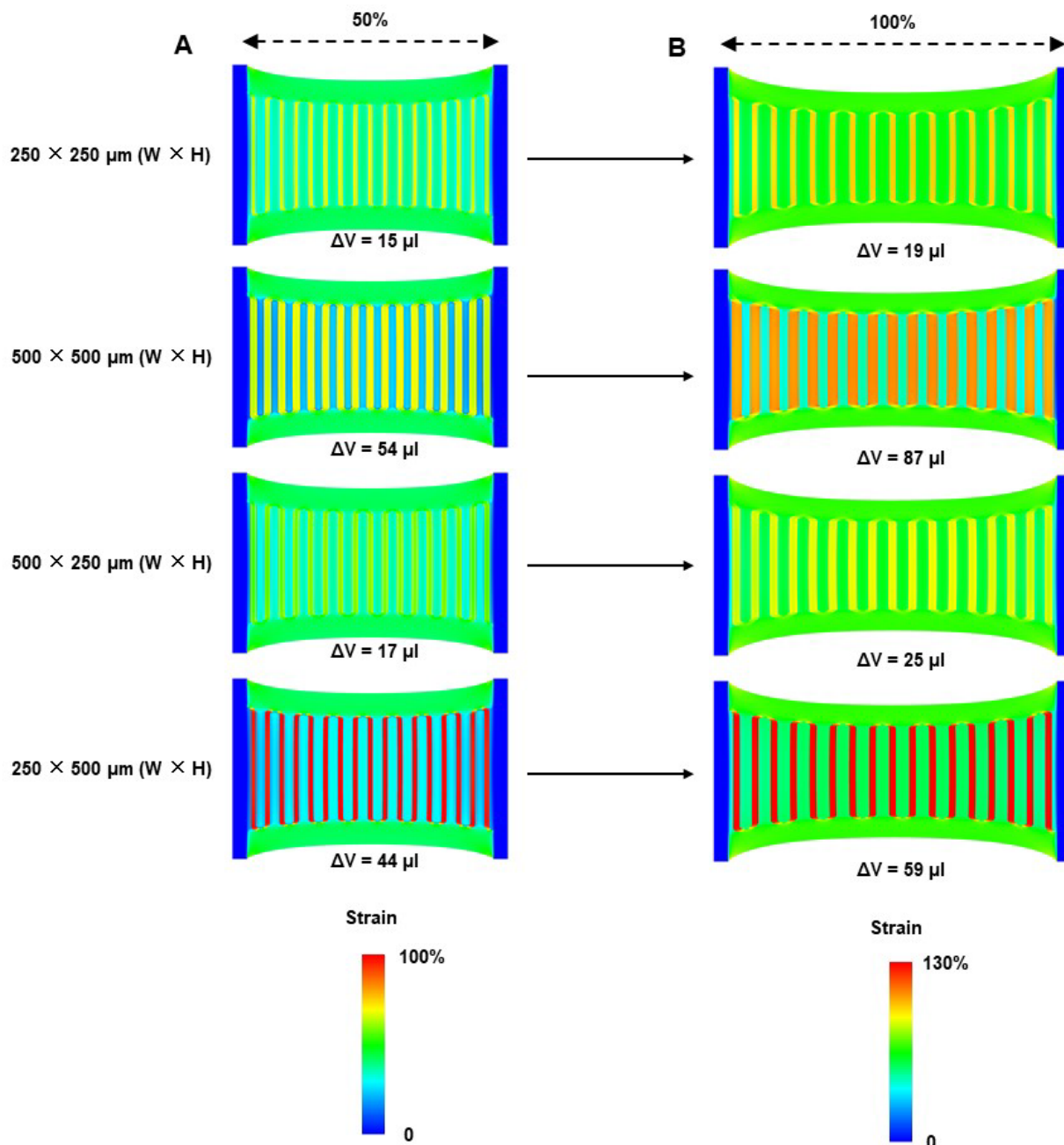
Supplementary Figure 4. Chloride measurements. A) A green molded layer provides a background for viewing both extent of fluid ingress via the microstructural optics as well as for colorimetric detection of sweat chloride via a reaction with silver chloranilate. Scale bar: 1 cm. B) Images of devices filled with reference chloride concentrations for calibration. C) A 24-panel color card is placed next to the device to enable color calibration in post-processing. D) a^* and b^* values for reference chloride measurements (LAB color space). Scale bar: 1 cm. D) Representative images of an on body chloride trial from the left and right volar forearms of a subject. F) Colorimetric detection of chloride sweat levels closely match those provided by a chloridometer. The LAB value represents the scaler projection of the measured color value onto the calibration curve in $a^* b^*$ space as shown in panel D. The error bars indicate standard deviation.



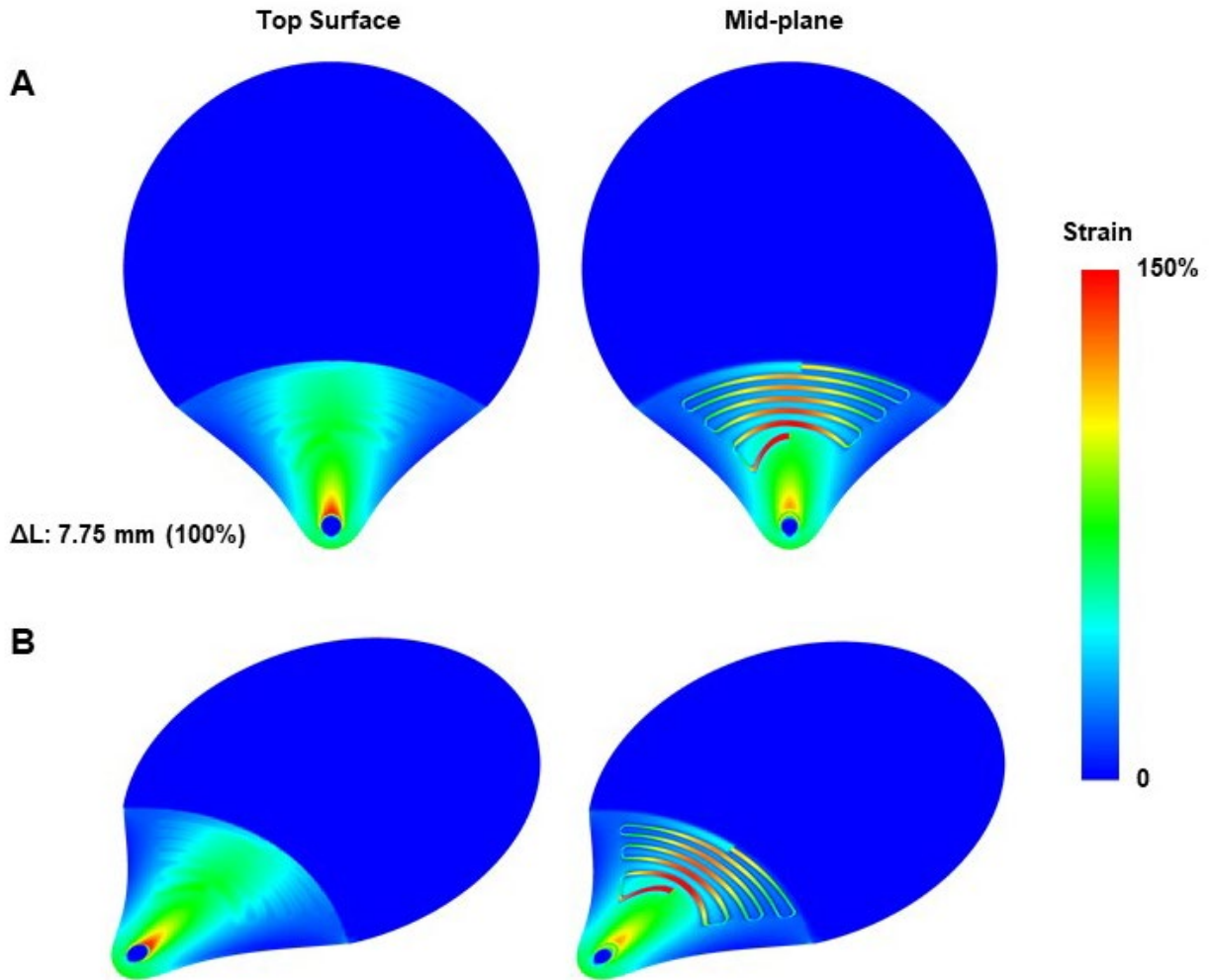
Supplementary Figure 5. Elastomeric pinch valve repeatability. A) Micrographs of an elastomeric pinch valve undergoing a burst pressure test. Before bursting (left), after bursting (center), and after resetting (right). No residual water droplets are observable due to the hydrophobicity of the PDMS. Scale car: 200 μm . B) No significant changes in burst pressure are observed for 20 cycles, or after an additional three cycles of 1 min hold. C) No significant changes in valve morphology are observed after cyclic burst pressure testing. Scale bar: 100 μm .



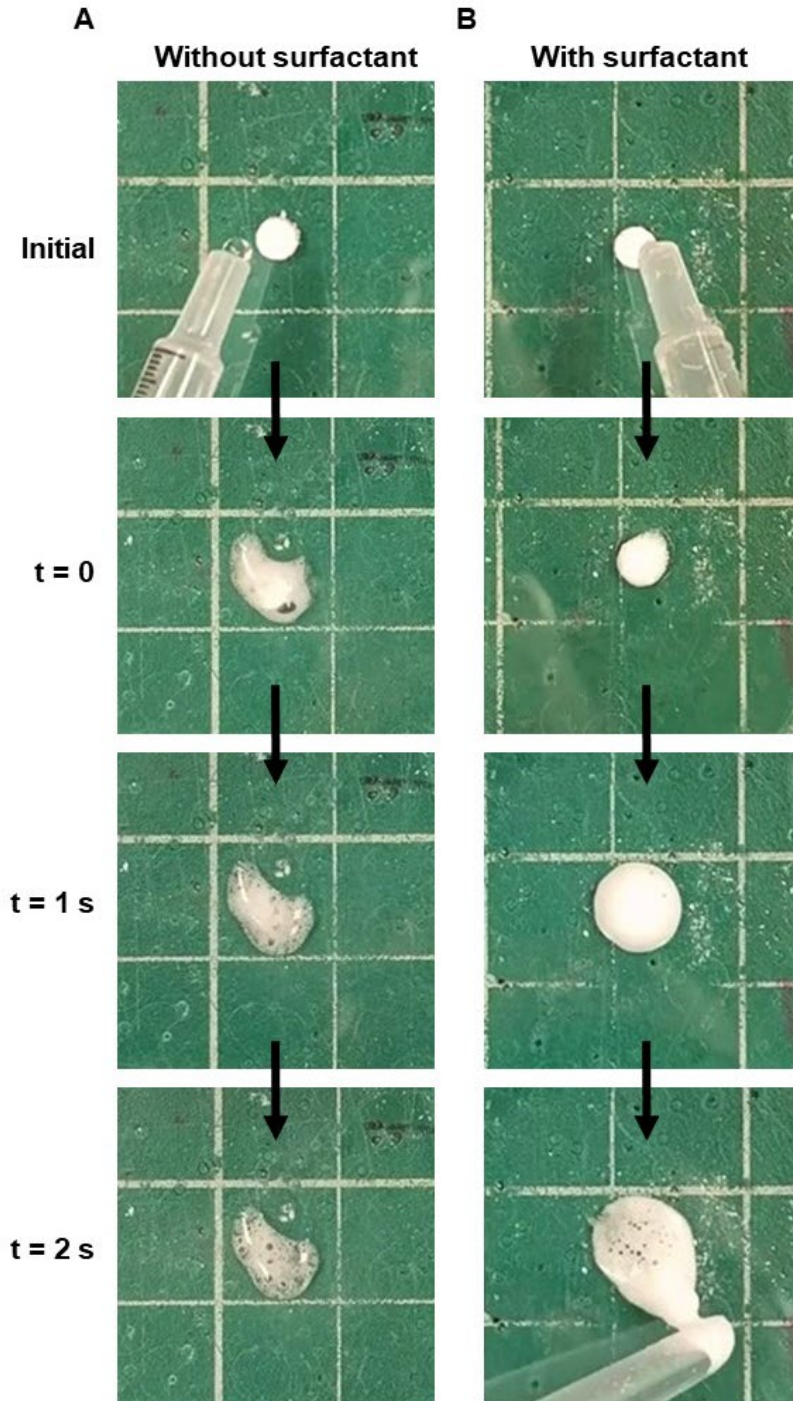
Supplementary Figure 6. Structure geometries for systematic tests of the microfluidic components and systems. A) Valve burst pressure tests. Scale bar: 10 mm. B) Pump tests. Scale bar: 20 mm. C) Purge tests. Scale bar: 20 mm.



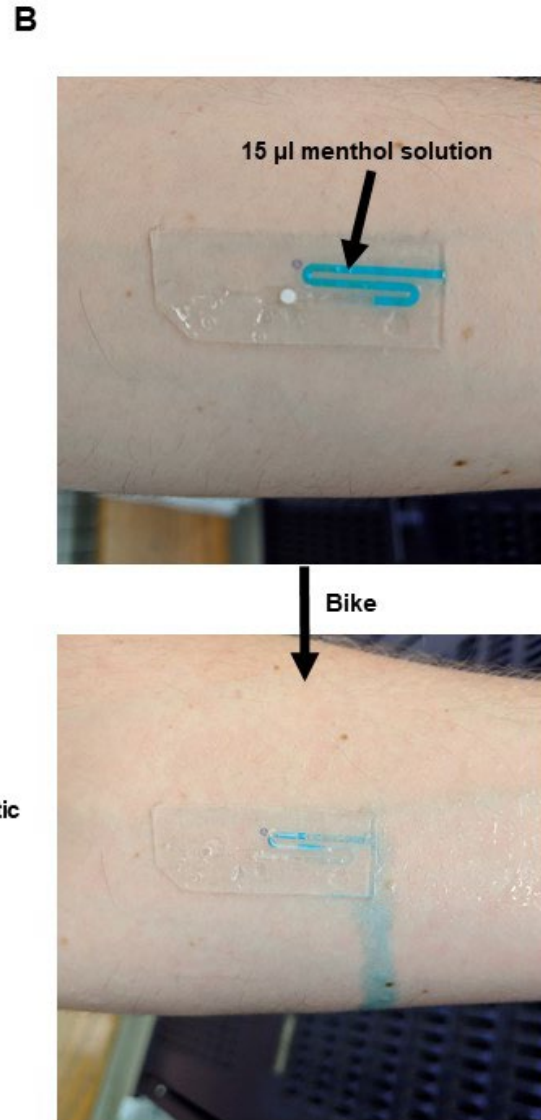
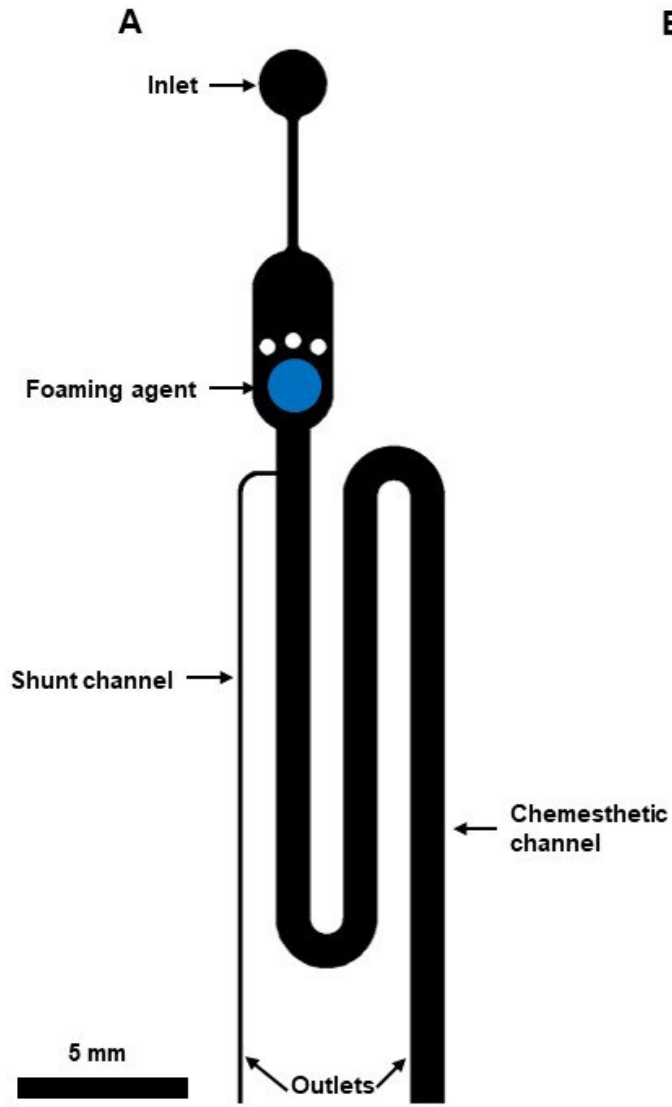
Supplementary Figure 7. 3D FEA of suction pump test structures. A) 50% strain. B) 100% strain. ΔV = volume change.



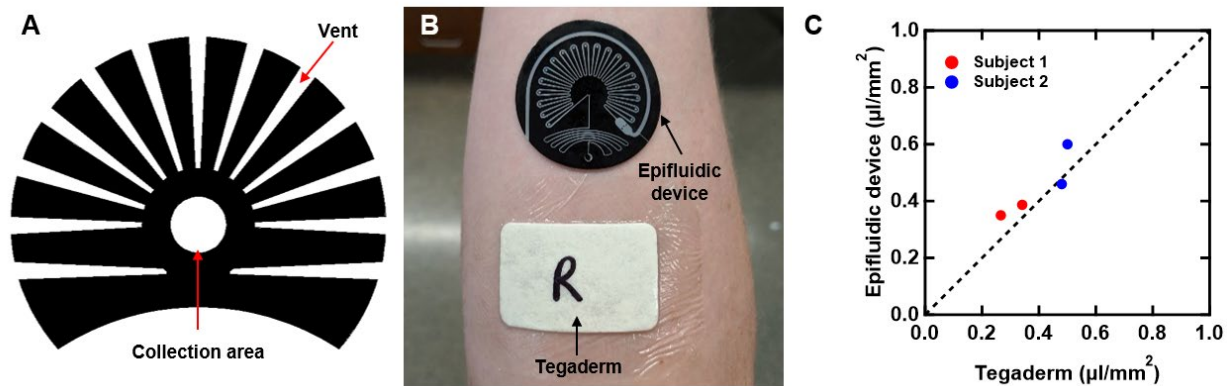
Supplementary Figure 8. 3D FEA of curved suction pump. A) Top view. B) Oblique view. ΔL = displacement.



Supplementary Figure 9. Effect of surfactant on foaming behavior of the effervescent tablet. A) Images of a 1 mg tablet of sodium bicarbonate: citric acid (1.2:1 wt:wt) reacting with a droplet of water. B) Images of a 1 mg tablet of sodium bicarbonate: citric acid (1.2:1 wt:wt) with an additional 3wt% polysorbate 20 reacting with a droplet of water. Scale bar: 5 mm.



Supplementary Figure 10. Chemesthetic trials. A) Epifluidic test structures for on-body chemesthetic tests. Scale bar: 5 mm. B) Representative results for a chemesthetic trial of menthol. Scale bar: 10 mm.



Supplementary Figure 11. Effect of patterned adhesive and compensatory sweating. A) Adhesive pattern including radial vents. B) An epifluidic device and Tegaderm absorbent pad mounted on the volar forearm. Scale bar: 2 cm. C) Areal sweat volume for epifluidic devices as compared to Tegaderm absorbent pads for two subjects.